Available online at www.sciencedirect.com
SCIENCE DIRECT®
Agricultural and Forest Meteorology 123 (2004) 201–219
AGRICULTURAL AND FOREST METEOROLOGY
www.elsevier.com/locate/agrformet

Sensitivity and uncertainty of the carbon balance of a Pacific Northwest Douglas-fir forest during an El Niño/La Niña cycle

Kai Morgenstern [a,*], T. Andrew Black [a], Elyn R. Humphreys [a], Timothy J. Griffis [b], Gordon B. Drewitt [c], Tiebo Cai [a], Zoran Nesic [a], David L. Spittlehouse [d], Nigel J. Livingston [e]

[a] *Biometeorology and Soil Physics Group, Faculty of Agricultural Sciences, University of British Columbia, 2357 Main Mall, Vancouver, BC, Canada V6T 1Z4*
[b] *Department of Soil, Water and Climate, University of Minnesota, St. Paul, MN, USA*
[c] *Department of Land Resource Science, University of Guelph, Guelph, Ont., Canada*
[d] *British Columbia Ministry of Forests, Research Branch, Victoria, BC, Canada*
[e] *Department of Forest Biology, University of Victoria, Victoria, BC, Canada*

Received 11 June 2003; received in revised form 26 November 2003; accepted 2 December 2003

Abstract

The annual net ecosystem productivity (F_{NEP}) of a second-growth Douglas-fir stand established in 1949 on the Canadian West Coast varied considerably over the 4-year period between 1998 and 2001. This period included the El Niño/La Niña cycle during the northern hemispheric winters of 1997/1998 and 1998/1999, offering a unique opportunity to study how a typical forest ecosystem in the Pacific Northwest reacts to interannual climate variability. This was possible even though annual F_{NEP} values calculated from eddy covariance (EC) measurements of CO_2 fluxes were subject to biases. These were largely due to the failure of the EC method to accurately measure losses of CO_2 under low turbulence conditions at night, which caused F_{NEP} overestimates of as much as 90 g C m^{-2} per year. As these biases were largely unaffected by interannual climate variability, it was possible to reliably quantify interannual differences in F_{NEP} estimates if they were larger than random variability, which was estimated to be ±30 g C m^{-2} per year at most. Interannual differences were mainly due to differences in ecosystem respiration (R) between the 4 years. In the year following the 1997/1998 El Niño, high air temperatures led to the highest annual R of the 4 years, while annual gross ecosystem photosynthesis (P) was only slightly higher than normal. This resulted in 1998 having the lowest F_{NEP} (270 g C m^{-2} per year) of the 4 years. For 1999, a cool and cloudy La Niña year, F_{NEP} was 360 g C m^{-2} per year, much higher than 1998, but somewhat lower than the last 2 years, for which F_{NEP} values were 390 and 420 g C m^{-2} per year, respectively.

Keywords: Net ecosystem productivity; Douglas-fir; Carbon balance; Ecosystem photosynthesis; Ecosystem respiration; Eddy covariance; Error analysis

1. Introduction

Terrestrial ecosystems play a dynamic role in the global carbon (C) cycle. Future climate change scenarios are widely predicted to be characterized by

* Corresponding author. Tel.: +1-604-822-9138; fax: +1-604-822-2184.
E-mail address: kai.morgenstern@ubc.ca (K. Morgenstern).

0168-1923/$ – see front matter © 2004 Elsevier B.V. All rights reserved.
doi:10.1016/j.agrformet.2003.12.003

changing precipitation regimes and increased surface temperatures as a result of an increase in atmospheric greenhouse gases (Cubasch et al., 2001; Mitchell et al., 2001). A complete understanding of the mechanisms involved in C cycling in terrestrial ecosystems is required to determine how the C budgets of these systems will respond to changes in climate. To achieve this, it is necessary to quantify the functional responses of major ecosystems to current climate conditions and their variations. At present, there is mounting evidence that terrestrial ecosystems in the northern hemisphere have, in the last two decades, represented net C sinks (Keeling et al., 1996; Prentice et al., 2001; Randerson et al., 1999). For the northern extratropical regions, recent estimates of total sink strength are about 1.5–4.3 Pg C per year (Schimel et al., 2001).

While there is ongoing debate about which factors are the cause of the observed variations in annual C sequestration (Jarvis et al., 2001; Piovesan and Adams, 2000; Valentini et al., 2000), long-term CO_2 flux measurements have confirmed that some temperate (e.g., Barford et al., 2001; Pilegaard et al., 2001) as well as boreal forests (e.g., Griffis et al., 2003; Lloyd et al., 2002) are C sinks. However, several northern forests have been identified as weak C sources, especially where growing season length limits ecosystem photosynthesis (P), as is the case with boreal evergreen coniferous forests in Manitoba and Sweden (Goulden et al., 1997; Lindroth et al., 1998). These divergent findings emphasize the need to determine current C uptake capacities of forests with different ecophysiological characteristics and in diverse climatic conditions. Furthermore, El Niño events, which lead to a marked change in weather patterns throughout the western part of the Americas, have been shown to enhance the rate of increase in atmospheric CO_2 concentration in the order of >1 Pg C per year compared to non-El Niño years (Prentice et al., 2001). Inversion analysis of atmospheric CO_2 concentrations and the isotopic signature of CO_2 for these events suggest that terrestrial ecosystems, mainly in the tropics, are largely responsible for this increase. The impact of El Niño on the carbon balance of terrestrial ecosystems along the Pacific Coast is currently poorly understood.

Pacific coastal forests of the northwestern United States and Canada cover approximately 10^5 km^2 between Oregon and Alaska and likely play a significant role in the global carbon cycle. The climate of the Pacific Northwest is characterized by relatively mild winters with high precipitation and moderately warm, dry summers providing a favorable environment for forest growth. Forests in the Pacific Northwest are dominated by evergreen coniferous trees, which under these climatic conditions have a competitive advantage over deciduous trees because of their ability to photosynthesize through the mild and wet fall to spring period. The reduced rainfall during summer distinguishes this coastal climate from most other temperate regions in Europe, eastern Asia, and the east coast of the United States, where precipitation is relatively constant throughout the year (Waring and Franklin, 1979).

To date, only a limited number of studies have provided estimates of forest productivity in the Pacific Northwest. For a transect of mature stands from the coast to sub-alpine forests in Oregon, Gholz (1982) estimated above-ground net primary productivity as between 400 and 1500 g C m^{-2} per year. High productivities have also been reported for two 40-year-old Douglas-fir stands (*Pseudotsuga menziesii* (Mirb.) Franco) in Washington State, USA, where estimates of above-ground net primary productivity were 640 and 370 g C m^{-2} per year while total net primary productivity was estimated to be 890 and 770 g C m^{-2} per year (Keyes and Grier, 1981). Along the coast, studies of C exchange for Douglas-fir stands included short-term measurements of above-canopy CO_2 fluxes in juvenile stands during the summer (Price and Black, 1990, 1991) and long-term monitoring of CO_2 fluxes above an old-growth stand in southern Washington State (Falk et al., 2002). In the latter, observed net ecosystem productivity (F_{NEP}) ranged from −50 to 210 g C m^{-2} per year over a 3-year period, i.e., varying from a weak source to a moderate sink. Warm weather significantly enhanced ecosystem respiration (R) and was responsible for this considerable variation. A long-term study of the C balance of ponderosa pine (*Pinus Ponderosa* Dougl. ex P. and C. Laws) is monitoring CO_2 exchange above a mature stand in coastal Oregon (Anthoni et al., 1999, 2002). Estimates of F_{NEP} of this stand, which is located in a semiarid environment, were about 300 g C m^{-2} per year and growing season R was strongly affected by water availability. Comparing two summers, R was shown to increase in the wetter year, reducing F_{NEP} (Anthoni et al., 1999).

This study reports measurements of F_{NEP} of a second-growth Douglas-fir stand established in 1949 on the east coast of Vancouver Island, Canada, during 4 years: 1998–2001. The measurement period includes the El Niño/La Niña cycle during the northern hemispheric winters of 1997/1998 and 1998/1999. In the Pacific Northwest, El Niño events typically induce mild winters followed by unusually warm spring months and dry summers, while La Niña years are characterized by wet winters and relatively cool and cloudy conditions in the following spring and summer (Shabbar et al., 1997; Shabbar and Khandekar, 1996). This departure from the regular temperature and precipitation pattern provides an opportunity to investigate the sensitivity of P and R to climate variations and how these fluxes impact annual F_{NEP} of a Douglas-fir forest typical of the region.

To gain confidence in estimates of annual F_{NEP} and its interannual variability, errors in the eddy covariance (EC) measurements of CO_2 fluxes used to obtain F_{NEP} must be evaluated. Moncrieff et al. (1996) and Goulden et al. (1996) considered random and bias errors of long-term C uptake calculated from EC data, while Falge et al. (2001) gave a detailed account of the effect of gap filling flux data using simple empirical methods. In this paper, we focus on biases introduced by the methods used to analyze annual CO_2 exchange measurements. For example, criteria for selecting cases with sufficient atmospheric turbulence vary, data may or may not be corrected for energy balance closure, and various procedures may be used for gap filling. All these variations cause systematic biases that cannot be described by confidence intervals since uncertainty in the results is not due to random noise in the measurements but to the uncertainty about the correct method of analysis. We follow Barford et al. (2001) in bracketing the systematic bias by giving annual sums for several combinations of possible steps in the analysis. This enables us to compare the effect of different methods of analysis and helps to focus research on the steps in the analysis associated with the largest uncertainties.

The objectives of this paper are to (1) evaluate the importance of systematic biases associated with deriving annual estimates of F_{NEP} from EC data, (2) determine the responses of P and R to environmental variables and the extent to which these responses change from year to year, and (3) explain the intra- and interannual variations of F_{NEP} in terms of the contributions of P and R.

2. Site and Instrumentation

2.1. The Site

The study site is located 10 km SW of Campbell River on the east coast of Vancouver Island, BC, Canada (49°52′N, 125°20′W), at an elevation of 300 m above sea level. It is part of the seasonal dry variety of the temperate rain forest that covers much of North America's Pacific Northwest. Its biogeoclimatic characterization is very dry maritime with Douglas-fir succeeding to coastal western hemlock (Meidinger and Pojar, 1991). Logging in the area began at the turn of the twentieth century. Stands that were not harvested were lost in the Sayward Fire of 1938. At the time, the majority of stands regenerated naturally, with stand ages varying according to the sites ability to regenerate, while some were planted by conscientious Mennonite objectors of WWII who had settled in the area. According to forest inventories of TimberWest Forest Corp., the land owner, the site was planted with Douglas-fir seedlings in 1949. Approximately, 860 ha of forest, including the research site, were fertilized by helicopter in 1994 with urea at an application rate of 200 kg N ha^{-1}. This has been the only fertilization application to date (B. Grutzmacher, personal communication).

The stand covers an area of 130 ha and is surrounded by Douglas-fir stands 20–60 years of age. It stretches for at least 400 m from the meteorological tower in all directions, extending to 700 m in the north-east and south-west quadrants. These include the prevailing summer daytime and nighttime wind directions, east–north–east and west–south–west, respectively. This wind direction pattern is a result of katabatic and anabatic flows caused by the north-east facing terrain with a slope of 5–10° and a complementary land–sea circulation, a result of the proximity of Georgia Strait located about 9 km east of the site.

The forest consists of 80% Douglas-fir (*Pseudotsuga menziesii* var *menziesii* (Mirb.) Franco), 17% western redcedar (*Thuja plicata* Donn ex D. Don) and 3% western hemlock (*Tsuga heterophylla* (Raf.) Sarg.). The understory is sparse, mainly

consisting of salal (*Gaultheria shallon* Pursh.), Oregon grape (*Berberis nervosa* Pursh), vanilla-leaf deer foot (*Achlys triphylla* (Smith) DC), and various ferns and mosses. In 1998, the mean stand density was 1100 stems ha^{-1} (95% confidence interval (CI): 950–1280 stems ha^{-1}), tree heights ranged from 30 to 35 m, and the mean tree diameter at breast height (DBH) was 29 cm (95% CI: 26–32 cm). The leaf area index (projected area basis) was estimated to be 9.1 m^2 m^{-2} (Gilbert Ethier, personal communication). The site index was 35 with a mean annual increment of 12.1 m^3 ha^{-1} (expected tree height in meters and mean annual volume increment per hectare for a 50-year-old coastal Douglas-fir stand, Humphreys et al., 2003). The soil at the site is a humo-ferric podzol with a gravelly sandy loam texture and a surface organic layer averaging 3 cm, but ranging from 1 to 10 cm in depth. The total soil C content to 1 m was 11.5 kg C m^{-2}, of which 2.5 kg C m^{-2} was in the surface organic layer. See Drewitt et al. (2002) for a more detailed description of soil properties.

2.2. Eddy flux measurements

Half-hour fluxes of CO_2, water vapor and sensible heat above the canopy were measured continuously using the EC technique starting in September 1997. A 45 m tall, 51 cm triangular open-lattice type tower provided support for the sensors. The EC instruments were mounted on the flux tower at a height of 43 m and consisted of a three-dimensional sonic anemometer-thermometer (SAT) (model 1012R2A up to March 2001, then model 1012R2, Gill Instruments, Lymington, UK) and a closed-path infrared gas (CO_2/H_2O) analyzer (IRGA) (model LI-6262, LI-COR Inc., Lincoln, NE, USA). The IRGA was maintained in a temperature-controlled box mounted 2 m lower than the SAT and on the opposite site of the flux tower. It was operated in absolute mode with nitrogen gas scrubbed to remove water vapor and CO_2 flowing through the reference cell at 60–80 cm^3 min^{-1}. Air was drawn from 30 cm below the center of the SAT array into the IRGA sample cell through a 4.2 m-long heated sampling tube (Dekoron type 1300, 4.0 mm inner diameter (i.d.), Cable USA, Cape Coral, FL, USA) and a filter located in the temperature controlled box (model ACRO 50, Gelman Sciences, Ann Arbor, MI, USA). A flow rate of 9.5 l min^{-1} was maintained using a linear AC pump (model SPP-15EBS-101 Gast Manufacturing Inc., Benton Harbor, MI, USA) located at the base of the tower. Delay times for the CO_2 and water vapor mixing ratios calculated using the SAT temperature were about 0.8 and 1 s, respectively.

A solenoid-valve system was used to automatically zero and calibrate the gas-analysis system once a day at midnight. This was done by releasing, first, nitrogen and then CO_2 in dry air calibration gas through a tee at the entrance of the sampling tube, causing almost no pressure change in the sample cell (Chen et al., 1999). The calibrations proved to be stable under field conditions (typically less than 0.5% variation in the span and less than 1 μmol mol^{-1} variation in the zero-offset measured in the field over the course of a year). The calibration gas cylinders were calibrated in the laboratory using standards provided by the Canadian Greenhouse Gases Measurement Laboratory, Meteorological Service of Canada, Downsview, Ont., Canada. CO_2 mixing ratios of the cylinders used over the course of the 4 years of measurements varied between 358 and 365 μmol mol^{-1}.

The analog IRGA signals required for EC calculations were filtered using a low-pass R–C analog filter (cut-off frequency 50 Hz) to minimize aliasing and then sampled by a data-acquisition system (DAS) (model DaqBook/200, IOtech Inc., Cleveland, OH, USA), equipped with an analog-to-digital converter (16 channels, 16 bit), at a frequency of 125 Hz. To match the non-adjustable sampling speed of the digital SAT output, the analog signals were subsequently down-sampled to 20.83 Hz after applying a digital low-pass filter (cut-off frequency 10 Hz) to the signals. The digital output from the DAS and the SAT were transferred to a PC via the parallel and serial ports, respectively, and written into output files every 30 min. On-line flux calculations were performed by the PC at the site (see below) using software written in MATLAB (The MathWorks Inc., Natick, MA, USA).

2.3. Storage change in the air column

Change in the storage of CO_2 in the air column below the EC measurement level was measured using a four-level profile sampling system, initially with a model LI-6262 IRGA for 1 month in the summers of 1999 and 2000. Continuous measurements started in

June 2001 with a model LI-800 IRGA (LI-COR Inc.). Air was drawn sequentially down sample tubes (Dekoron type 1300, 20 mm i.d.) at a flow rate of 22 l min^{-1} for 7.5 min, providing a single measurement for each sampling height every half-hour. Inlet funnels at the 42, 27, 12, and 2 m heights were equipped with variable lengths of 4 mm i.d. Dekoron tube to give the same pressure drop for all sampling tubes. A sample was diverted into the LI-800 at a flow rate of 0.8 l min^{-1}. After flushing the IRGA for 60 s an average CO_2 mole fraction was calculated from measurements in the following 390 s. The IRGA was calibrated daily at midnight by flushing nitrogen and calibration gas through the 2 m height sampling tube.

2.4. Supporting measurements: climate and environmental variables

A pyranometer (model CM 5, Kipp and Zonen Laboratory) was used to measure downwelling solar radiation, and a quantum sensor (model 190SB, LI-COR Inc.) measured downwelling photosynthetically active radiation (Q). Net radiation (R_n) was measured by a model S-1 net radiometer (Swissteco Instruments, Oberriet, Switzerland) and, since August 1999, by a four-way radiation sensor (model CNR 1, Kipp and Zonen Laboratory, Delft, The Netherlands) consisting of two pyranometers (model CM 3) and two pyrgeometers (model CG 3) monitoring upwelling and downwelling solar and longwave radiation at the 41 m height. The S-1 was found to give 4% lower R_n than the CNR 1. Furthermore, a comparison with the CM 5 showed a drift in the S-1 over the 4 years, while a comparison of the CM 5 and the quantum sensor showed no systematic variation over the measurement period. The S-1 measurements were adjusted to give a consistent relationship with measured downwelling solar radiation, leading to a 2–6% increase in net radiation for 1999–2001.

Soil surface heat flux (G) was obtained at three locations from soil heat flux plates (model F, Middleton Instruments, Melbourne, Australia) at the 3 cm depth and corrected for the heat storage change in the soil layer above. Air temperature and relative humidity sensors (model HMP-35C, Vaisala Oyj, Helsinki, Finland) were installed at the 4, 27 and 40 m heights. Additional thermocouples provided air temperature measurements at eight different heights on the tower, soil temperature measurement at five depths between 2 and 100 cm and tree bole temperature measurements in two trees. Soil water content was measured by soil moisture reflectometers (model CS-615, Campbell Scientific Inc., Logan, UT) at four depths between 2 and 100 cm and by 11 time domain reflectometry stations. These extended up to 150 m upwind of the tower and integrated the top 30 and 76 cm of the soil (Humphreys et al., 2003) and, beginning in 2001, the top 20, 60 and 90 cm. Soil water matric potential (Ψ) was calculated from these measurements using soil water retention curves measured in the laboratory and confirmed using occasional measurements of predawn twig water potential (Humphreys et al., 2003). Rain was monitored by two tipping bucket rain gauges (model 525I, Texas Electronics, Dallas, TX, USA, and model 2501, Sierra Misco, Berkeley, CA, USA) at the 24 m height. From these measurements, the total rate of change in energy storage (J), composed of the sensible heat storage in the air column beneath the EC instrumentation and the biomass, and the latent heat storage in the air column, were calculated using the algorithm described in Humphreys et al. (2003). The available energy was calculated as $R_a = R_n - G - J$.

3. Methods

3.1. Calculation of turbulent fluxes

Prior to calculating eddy fluxes, measured mole fractions χ_x (mol per mol of moist air, x denoting either v for water vapor or C for CO_2) were converted to mole mixing ratios s_x (mol mol^{-1} of dry air). Wind speed vectors and fluxes were expressed using a rotated reference frame determined on a half-hourly basis using the procedure of Tanner and Thurtell (1969). In this frame, the mean vertical ($\bar{w}$) and lateral ($\bar{v}$) velocity components as well as the covariance between these velocity components ($\overline{w'v'}$) are zero, where the overbar and prime indicate the temporal mean and fluctuations around the mean, respectively. The latter were calculated by subtracting the half-hourly mean from the instantaneous values, i.e., by block averaging. For our Douglas-fir site in the year 2000, the rotated CO_2 fluxes were only 2% larger than the unrotated fluxes (median of the relative differences). This

suggests that the application of the more rigorous approach of Finnigan et al. (2003) that defines the rotated reference frame for fluxes on time periods as long as months will not lead to large changes in the magnitude of fluxes.

CO_2 fluxes were calculated for half-hourly intervals as $F_C = \bar{\rho}_a \overline{w's'_C}$, where $\bar{\rho}_a$ is the mean molar density of dry air and $\overline{w's'_C}$ is the covariance between the rotated w and s_C (Webb et al., 1980), with positive covariances corresponding to upward transport. Evaporative fluxes were calculated as $E = \bar{\rho}_a \overline{w's'_v}$, from which the latent heat fluxes were derived as λE, where λ is the latent heat of vaporization. Similarly, sensible heat fluxes were calculated as $H = (c_{Pa}\bar{\rho}_a + c_{Pv}\bar{\rho}_v)\overline{w'T'_a}$, where $\bar{\rho}_v = \bar{s}_v\bar{\rho}_a$, c_{Pa} and c_{Pv} are the specific heats of dry air and water vapor at constant pressure, respectively, and $\overline{w'T'_a}$ is the covariance of the rotated vertical wind speed and air temperature (T_a). As the anemometer only provided sonic temperature (T_{sonic}), which was derived from the measured speed of sound assuming that the air was dry, T_a was calculated as $T_a = T_{sonic}(1 + 0.32\chi_v)^{-1}$ (Kaimal and Finnigan, 1994).

3.2. Calculation of storage fluxes and net ecosystem exchange

The rate of change in CO_2 storage (the "storage flux") in the air column below the EC measurement level was calculated from the mole fraction measurements of the LI-800 IRGA sampling the four profile levels using

$$F_S^p = \sum_{j=1}^{4} \Delta h_j \bar{\rho}_j \frac{\Delta \bar{\bar{\chi}}_{C,j}}{\Delta t} \quad (1)$$

where Δh_j is the depth of the air layer j centered around each measurement height, and $\bar{\rho}_j$ is the mean air density in the layer. A centered running mean $\bar{\bar{\chi}}_{C,j,i} = (\bar{\chi}_{C,j,i-1} + \bar{\chi}_{C,j,i} + \bar{\chi}_{C,j,i+1})/3$ was used to reduce noise due to the single 390 s interval representing each layer for the ith half-hour. Then, $\Delta\bar{\bar{\chi}}_{C,j}/\Delta t$ was calculated for half-hour i using $\Delta\bar{\bar{\chi}}_{C,j,i}/\Delta t = (\bar{\bar{\chi}}_{C,j,i+1} - \bar{\bar{\chi}}_{C,j,i-1})/3600$ s.

Alternatively, storage was calculated by assuming the mixing ratio measurement of the LI-6262 EC IRGA was representative of the whole air column (Hollinger et al., 1994)

$$F_S^{EC} = h_m \bar{\rho}_a \frac{\Delta \bar{s}_C}{\Delta t} \quad (2)$$

where h_m is the measurement height and the change in mixing ratio $\Delta\bar{s}_C$ was calculated as the difference between $\bar{s}_C$ of the following and previous half-hours. The use of mixing ratio and dry air density avoided apparent changes in CO_2 storage due to the addition of water vapor to the air column. The use of total air density and mole fraction in Eq. (2) resulted in a 2% reduction of storage values, suggesting an increase of the same magnitude would have occurred had mixing ratio measurements been available for use in Eq. (1).

As F_S^p was not measured throughout the measurement period, half-hourly net ecosystem exchange of C (F_{NEE}) was calculated as

$$F_{NEE} = F_C + F_S^{EC} \quad (3)$$

for the entire measurement period to avoid systematic differences in F_{NEE} between years. Here, positive values of F_{NEE} correspond to C losses from the ecosystem. Mean monthly diurnal courses of the two storage estimates together with the F_{NEE} values calculated from them are shown in Fig. 1 for July 2001. F_S^{EC} and F_S^p showed good agreement at night, during the early morning and during the early afternoon. Only during mid-morning (around 09:00 PST) and mid-afternoon (around 16:00 PST) did F_S^{EC} slightly underestimate the magnitude of F_S^p. Consequently, $F_C + F_S^p$ differed from F_{NEE} only during these periods. The difference was about 10% and therefore small enough to justify the use of F_S^{EC} in Eq. (3) to yield a consistent record of F_{NEE} for the 4 years of measurements.

3.3. Annual net ecosystem productivity

F_{NEP} was calculated as the integral of all half-hourly F_{NEE} values with the sign chosen to give positive values for C uptake by the ecosystem:

$$F_{NEP} = -\sum_{i=1}^{n} F_{NEE,i}\,\Delta t \quad (4)$$

where n is the number of half-hours, e.g., $n = 17{,}520$ for the full year, and $\Delta t = 1800$ s. Gaps in the annual

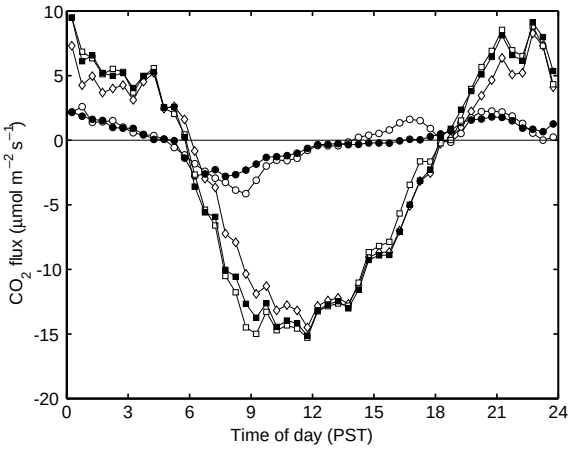

Fig. 1. Mean monthly diurnal courses of the storage fluxes calculated from the CO_2 concentration measured by the EC IRGA (F_S^{EC}, ●) and from the four-level CO_2 profile system (F_S^p, ○), the turbulent CO_2 flux F_C (◇) at the 43 m height, and the net ecosystem exchange (F_{NEE}) calculated as $F_C + F_S^{EC}$ (■) and $F_C + F_S^p$ (□) for July 2001. Standard deviations of the mean diurnal values of F_S^{EC} and F_S^p were less than 3 μmol m^{-2} s^{-1} for most of the day, decreased below 1 μmol m^{-2} s^{-1} during midday and reached as much as 5 μmol m^{-2} s^{-1} around 06:00 PST.

record of measured F_{NEE} were filled and measurements made under low atmospheric turbulence conditions at night were replaced using the following four steps:

1. Data under sufficiently turbulent conditions at night were selected when the friction velocity (u_*) was above a chosen threshold value (u_{*th}).
2. An exponential relationship was found between nighttime F_{NEE} selected in step 1 and soil temperature at the 5 cm depth and used to fill missing and rejected nighttime data and to calculate daytime respiration (R_d). When $T_a < -1\,^\circ$C, gaps in daytime data were also filled using this relationship, as photosynthesis was found not to occur below this temperature.
3. $P = -F_{NEE} + R_d$ was calculated from F_{NEE} measurements during the day.
4. A Michaelis–Menten relationship between P and Q was found and used to fill gaps in daytime data when $T_a > -1\,^\circ$C.

The gap filled values of F_{NEE}, R for both nighttime and daytime, and P were used to calculate annual and monthly totals of F_{NEP}, R, and P.

Observations of low half-hourly F_{NEE} measurements for low turbulence conditions at night were reported, for example, by Goulden et al. (1996), Blanken et al. (1998), Pilegaard et al. (2001), and Barford et al. (2001) and exclusion of these data from the analysis is common practice (see Falge et al., 2001 and Baldocchi, 2003 for discussions of this approach). Gaps resulting from this exclusion can be filled in a number of ways. For example, 29 studies published between 1993 and 2001 all used different methods to find a relationship between nighttime F_{NEP} and some temperature (step 2 above). Methods differed in the choice of temperature (soil or air), the degree of averaging (half-hourly, hourly, or all night), the choice of relationship (linear, exponential, logistic, or Arrhenius function), and the mathematical procedure used to find the best fit between the chosen relationship and the data. Different combinations of these choices lead to different values used to fill gaps in the data set and subsequently to differences in annual F_{NEP} for a single data set even when all other steps in the analysis are the same. Consequently, they are a source of bias. Falge et al. (2001) gave a comprehensive overview of the impact of various gap filling procedures on the values of annual F_{NEP}.

3.4. Ecosystem respiration and photosynthesis

The most common choice of functional relation describing the relationship between temperature and R is the exponential function (see, e.g., Black et al., 1996; Goulden et al., 1996 and others):

$$R = A\exp(BT) = R_{ref}\,Q_{10}^{(T-T_{ref})/10} \quad (5)$$

where R_{ref} is the respiration rate at a reference temperature T_{ref} (here 10 °C was used) and Q_{10} is the factor by which R increases for a 10 °C increase in temperature (Lloyd and Taylor, 1994). As an example, nighttime F_{NEE} measurements with $u_* > 0.3$ m s^{-1} for 2000 are plotted against soil temperature at the 5 cm depth in Fig. 2(a) together with a non-linear ordinary least squares (OLS) fit ($r^2 = 0.40$, $n = 2197$). It has been argued that the Arrhenius function $R = R_{ref}\exp(E_a/\Re((1/T_{ref}) - (1/T)))$, where E_a is the activation energy and $\Re$ is the gas constant, provides a better description of the physiological processes controlling R (Lloyd and Taylor, 1994). In the case

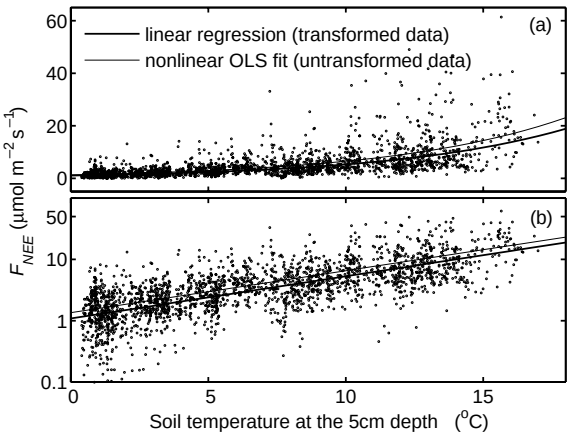

Fig. 2. (a) Relationship between nighttime net ecosystem exchange (F_{NEE}) measurements, representing nighttime respiration (R), and soil temperature (T_s) at the 5 cm depth together with an exponential relationship obtained by a non-linear OLS fit of an exponential function (thin line). (b) A logarithmic transformation of the F_{NEE} values allows the use of linear regression (thick line) and removes the inhomogeneous scatter of the data around the fitted function. Data are nighttime measurements from 2000 with $u_* > 0.3\,\mathrm{m\,s^{-1}}$ ($n = 2197$).

of the data in Fig. 2(a) a fit of an Arrhenius function is virtually indistinguishable from the exponential relationship and also gives $r^2 = 0.40$. Obviously, EC data is not suitable to decide which relationship describes respiration correctly because of the variability in F_{NEE} caused by atmospheric turbulence.

The scatter of the nighttime fluxes around the regression line varies with temperature (heteroscedasticity). When the biotic flux, or respiration rate, is small, atmospheric turbulence cannot cause large changes in the magnitude of F_{NEE}, yet large biotic fluxes can be significantly affected by the same level of turbulence and hence the expected variation of measured F_{NEE} is larger. As a non-linear OLS fit assumes homogeneous scatter in the data (Tabachnick and Fidell, 2001), this method should not be used to find the regression line. A logarithmic transformation of the data (Fig. 2(b)) removes the problem of inhomogeneous scatter and allows the use of a form of Eq. (5) that is linear in T:

$$\ln R = \ln A + BT = \ln\left(\frac{R_{\mathrm{ref}}}{Q_{10}^{T_{\mathrm{ref}}/10}}\right) + \frac{\ln Q_{10}}{10}T \quad (6)$$

Linear OLS regression was used to find the best fit. The requirement that only the dependent variable has errors was met since the random error of measured soil temperature was small compared to that of nighttime F_{NEE}. Fig. 2(b) demonstrates that the data are well described by Eq. (6) ($r^2 = 0.47$) and suggests that even observations above 50 $\mu\mathrm{mol\,m^{-2}\,s^{-1}}$ at the upper end of the temperature range are consistent with the variability observed over the whole range. At high temperatures, more CO_2 is respired into the canopy space and intermittent turbulent events that vent this space lead to a much greater random variability in the observed CO_2 fluxes. On a half-hourly time scale, nighttime fluxes associated with $u_* > 0.3\,\mathrm{m\,s^{-1}}$ were better correlated to 5 cm soil temperature than to air temperature ($r^2 = 0.41$ for regression of log-transformed F_{NEE} against air temperature). Therefore, the 5 cm soil temperature was used in finding the $R(T)$ relationship.

The most widely used relationship for describing the light response of P at the canopy scale (step 3 above) is the Michaelis–Menten function (e.g., Chen et al., 1999; Falge et al., 2001):

$$P = \frac{\alpha A_{\max} Q}{\alpha Q + A_{\max}} \quad (7)$$

where α is the quantum yield and $A_{\max}$ is the canopy photosynthetic capacity. Since the daytime data were also subject to inhomogeneous scatter, a linearization was attempted. Unfortunately, this did not solve the scatter problem as it led to $1/P = 1/A_{\max} + 1/(\alpha Q)$, which acted to increase variability for small values of P and Q. Hence, Eq. (7) with a non-linear OLS fit and Eq. (6) with a simple linear regression are used here to describe P and R, respectively.

Error estimates for the values of the parameter R_{ref} and Q_{10} in Eq. (6) were derived from the standard errors $\Delta(\ln A)$ and ΔB of the linear regression parameters (Squires, 1968) through Gaussian propagation of errors as

$$Q_{10} = (\exp B)^{10} \Rightarrow \Delta Q_{10} = 10(\exp B)^{10}\,\Delta B \quad (8)$$

$$R_{\mathrm{ref}} = \exp(\ln A)\exp(T_{\mathrm{ref}} B) \Rightarrow \Delta R_{\mathrm{ref}} = R_{\mathrm{ref}}\sqrt{(T_{\mathrm{ref}}\,\Delta B)^2 + (\Delta(\ln A))^2} \quad (9)$$

Errors in the parameters α and $A_{\max}$ in Eq. (7) were estimated by bootstrap Monte Carlo simulation (Manly, 1997). From the original data set of size n, n data points were randomly sampled with replacement (i.e., allowing repeated sampling of the same data point) and Eq. (7) was fitted to this resampled set. This procedure was repeated a hundred times to yield a

hundred estimates of α and A_{max}. The standard deviations of these hundred estimates were used as estimators of the standard deviation of the parameters given by the original fit.

Finding parameterizations of R for periods less than a whole year proved difficult. To establish a meaningful relationship, the temperature range covered by the data had to be sufficient to allow the relationship to emerge from the scatter in the data. For this, the difference in temperature needed to be at least 5 °C (see Fig. 2), precluding the use of periods shorter than approximately 3 months. The light response function, on the other hand, could be extracted from monthly data. However, the values of the parameters varied little over the course of the year, with the notable exception in September. As this deviation lasted for only a short time, we chose to establish functional relationships for gap filling on an annual basis for both P and R.

3.5. Evaluating random error and systematic biases

The random error ΔF_{NEP} of the annual F_{NEP} (Eq. (4)) was calculated as the random error of a sum (Squires, 1968) using random error estimates $\Delta F_{NEE,i}$ of the half-hourly $F_{NEE,i}$ values. Two random error estimates were employed: a 'worst case' estimate of $\Delta F_{NEE,i} = 10\,\mu mol\,m^{-2}\,s^{-1}$, which is the order of magnitude of midday fluxes, for all n measurements throughout the year (Eq. (10) below), and a 20% random error $\Delta F_{NEE,i} = 0.2|F_{NEE,i}|$ as suggested by Wesely and Hart (1985) (Eq. (11) below). This led to two random error estimates for the annual F_{NEP}:

$$\begin{aligned}\Delta F_{NEP} &= \sqrt{\sum_i^n (\Delta F_{NEE,i}\Delta t)^2} \\ &= \sqrt{\sum_i^n (10\,\mu mol\,m^{-2}\,s^{-1}\,\Delta t)^2} \\ &= 10\,\mu mol\,m^{-2}\,s^{-1}\,\Delta t\sqrt{n} \end{aligned} \quad (10)$$

$$\begin{aligned}\Delta F_{NEP} &= \sqrt{\sum_i^n (0.2|F_{NEE,i}|\Delta t)^2} \\ &= 0.2\sqrt{\sum_i^n (|F_{NEE,i}|\Delta t)^2} \end{aligned} \quad (11)$$

Eq. (10) shows that the random error of the sum of F_{NEE} values grows approximately as the square root of the number of values. The more realistic estimate Eq. (11) demonstrates that the random error will grow monotonically as more measurements are included.

Systematic biases of the analysis process were investigated by changing a single step in the standard method of analysis (steps 1–3 above). The change in annual F_{NEP} then served as a measure of the bias associated with the new method of analysis. Three systematic biases of the analytical procedure were investigated: (A) variation of u_{*th}, (B) correction for the lack of *energy balance closure*, and (C) correction for *photoinhibition* of R_d. To estimate bias A, u_{*th} was varied from 0 to $0.6\,m\,s^{-1}$ following Barford et al. (2001) who used the variation of annual F_{NEP} with u_{*th} to bracket its uncertainty. For bias B, the energy balance correction was derived from an orthogonal regression of $H+\lambda E$ against the available energy R_a, for nighttime data when $u_* > u_{*th}$ and all daytime data. Orthogonal regression was used here since it accounts for the error in the independent variable, R_a. To correct turbulent CO_2 fluxes for energy balance closure they were divided by the slope of the regression. A similar method was employed by Black et al. (2000). Twine et al. (2000) referred to this kind of adjustment as 'Bowen ratio closure' because the lack of energy balance closure is attributed to an error in the measurement of H and λE that is assumed to affect all turbulent fluxes in a similar way. This allows the Bowen ratio to be preserved and a correction factor can be derived for the sum of the turbulent heat fluxes and applied to the turbulent CO_2 flux as well. Blanken et al. (1998) showed that Bowen ratio closure markedly reduced half-hour to half-hour eddy flux variability and Twine et al. (2000) presented evidence that it improved the agreement of F_{CO_2} and λE with results from independent estimates. Nevertheless, Bowen ratio closure is not a widely accepted practice. Therefore, we assume that the energy balance correction adds to the overall uncertainty of the analysis and that the change in annual F_{NEP} estimates due to the application of Bowen ratio closure reflects the magnitude of this uncertainty. Bias C, the correction for photoinhibition of respiration, was introduced because it has been found that daytime leaf respiration is reduced compared to nighttime values (Brooks and Farquhar, 1985; Villar et al.,

1994). Janssens et al. (2001) suggested that R_d might be overestimated by as much as 15% if photoinhibition is neglected. Therefore, to estimate bias C, all estimates of R_d were reduced by 15% before calculating P.

4. Results and Discussion

4.1. Climate and meteorological conditions

The climate at the Douglas-fir site is characterized by an annual average temperature of 8.6 °C with an average annual precipitation of 1450 mm, approximately 75% of which occurs between October and March (Meteorological Service of Canada, 2002; see Fig. 3). Maximum air temperatures occur in July and August, when the mean monthly temperature reaches 16.9 °C, while minima usually occur during January, averaging 1.3 °C. Monthly average Ψ as in Fig. 3(b) shows that low precipitation during summer led to a dry period peaking in September, and ending in October with the onset of rainfall in autumn.

Following the typical pattern expected for an El Niño/La Niña cycle in the Pacific Northwest, spring and early summer temperatures in 1998 were above the long-term average resulting in an above-average mean annual temperature of 9.1 °C. The warm first half of that year combined with below-normal rainfall during the summer led to a severe late summer drought, as indicated by the low Ψ recorded in September. The coldest spring and summer temperatures of the measurement period occurred in 1999 following the La Niña in the previous winter, and consequently the mean annual temperature of 7.6 °C was well below normal. Late summer drought in 1999 was moderate due to the above average precipitation for much of the year. Annual courses of temperature and precipitation for 2000 and 2001 were closer to normal as were their mean annual temperatures of 8.2 and 8.1 °C. Late summer Ψ for these years was similar to 1999.

A comparison of Figs. 3(c) and 4(c) shows that monthly average soil temperature at the 5 cm depth closely followed the pattern of air temperature, both being highest in July or August. Q (Fig. 4(b)) reached a maximum value in June or July and was most variable between years in June with the lowest value occurring in 1999. Fig. 4(a) shows that monthly average u_* had a weak annual trend and dropped to 0.2 m s^{-1} in late summer when generally fair weather led to calm conditions. It was often greatest in early spring (February through April) when frontal passages dominate the weather pattern in the Pacific Northwest.

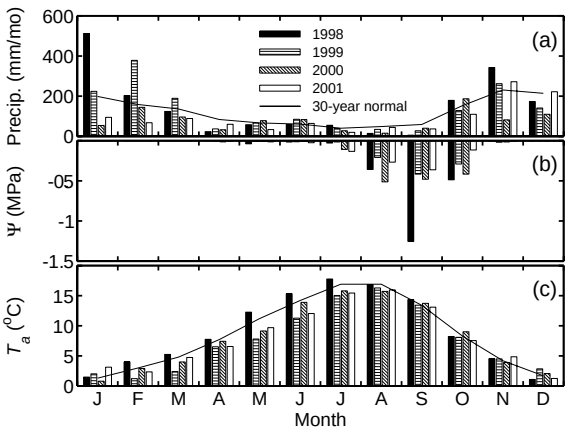

Fig. 3. (a) Monthly totals of precipitation, (b) monthly average soil water matric potential to 30 cm (Ψ), and (c) monthly average air temperature (T_a) at the 43 m height. Climate normals are for 1971–2000 from the Meteorological Service of Canada (2002) for Campbell River Airport, elevation 105 m, 10 km NE of the research site.

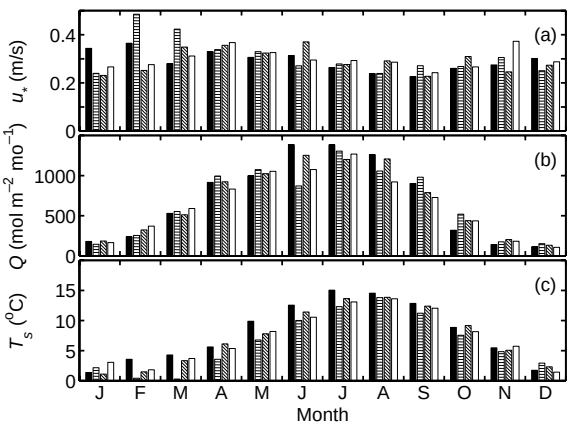

Fig. 4. (a) Monthly average friction velocity (u_*), (b) monthly downwelling photosynthetically active radiation (Q) totals, and (c) monthly average soil temperature (T_s) at the 5 cm depth. The legend is the same as in Fig. 3.

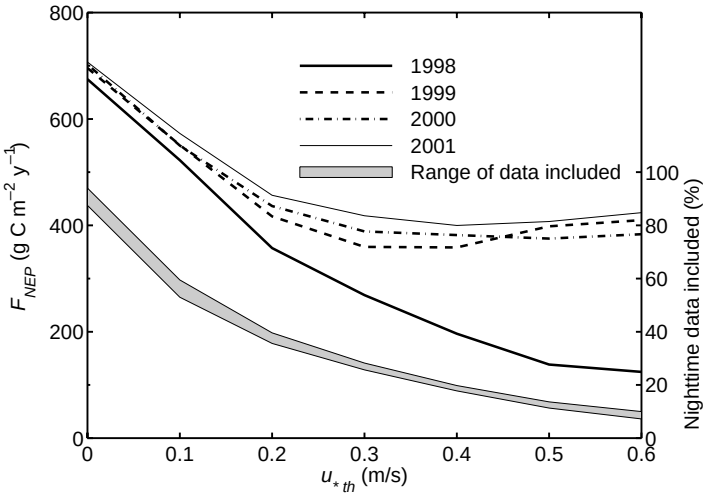

Fig. 5. Dependence of annual net ecosystem productivity (F_{NEP}) on threshold friction velocity threshold (u_{*th}) and the range of percentages of nighttime data included in the analysis.

4.2. Uncertainty in annual F_{NEP}

4.2.1. Systematic biases

Here, we follow Barford et al. (2001) in bracketing the systematic bias by giving annual F_{NEP} for the 4 years calculated using the standard method of analysis (steps 1–4) for varying u_{*th} (Fig. 5). The differences in annual F_{NEP} between years increased with increasing u_{*th} for $u_{*th} < 0.3\,m\,s^{-1}$. F_{NEP} in 1998 always had the lowest value, 2001 had the highest, and 1999 and 2000 were similar. In all years, annual F_{NEP} decreased with increasing u_{*th} to $0.3\,m\,s^{-1}$, when values leveled off for 1999, 2000, and 2001, but continued to decrease for 1998. Using $u_{*th} = 0.3\,m\,s^{-1}$, only about 25% of nighttime data (65% of all data) were acceptable for analysis. The variable behavior of annual F_{NEP} beyond $0.3\,m\,s^{-1}$ is due to the small number of data (Fig. 5). In 1998, isolated events with high nighttime fluxes at high u_* values led to increasing estimates of R and therefore decreasing F_{NEP} as u_{*th} increased, whereas, for example in 2000 (data in Fig. 2), relatively few high flux events occurred at high u_* values. This caused the R estimate to stabilize and consequently F_{NEP} to level off at high u_{*th}. We therefore chose $u_{*th} = 0.3\,m\,s^{-1}$ for the subsequent analysis. The dependence of half-hourly nighttime fluxes on u_* (e.g., Blanken et al., 1998; Pilegaard et al., 2001) for our site looks much like that reported by other authors and also suggests $u_{*th} = 0.3\,m\,s^{-1}$. Fig. 5 shows that u_{*th} values below $0.2\,m\,s^{-1}$ are clearly unacceptable, yet the choice of $u_{*th} = 0.3\,m\,s^{-1}$ is somewhat arbitrary. To characterize the range of uncertainty associated with u_{*th} we therefore also included $u_{*th} = 0.2\,m\,s^{-1}$ in the analysis.

A common criticism of gap filling data below u_{*th} is that it leads to 'double counting' of C that is respired at night and ejected from the canopy air space early in the morning (Aubinet et al., 2000). Yet, if Eq. (3) always accurately represented the biotic flux there would be no dependence of F_{NEE} on u_* and consequently no bias of the annual F_{NEP}. Yet, Fig. 5 shows such a bias. Furthermore, we do not observe the early morning spikes reported by other authors (e.g., Grace et al., 1995; Greco and Baldocchi, 1996; Yang et al., 1999) indicating that the C respired during low u_* conditions at night is lost from the system through non-turbulent transport. Hence, we feel that our gap filling approach does not lead to double counting.

Fig. 6 shows 5-day averages of F_{NEP} calculated using the standard method with $u_{*th} = 0.3\,m\,s^{-1}$ (Fig. 6(a)) and the difference between F_{NEP} calculated using the standard method and calculated using $u_{*th} = 0.2\,m\,s^{-1}$ (bias A, Fig. 6(b)). A positive difference (bias) indicates that an increase in u_{*th} reduces calculated F_{NEP} values. A reduction of fluxes occurs mainly during the summer months because of the

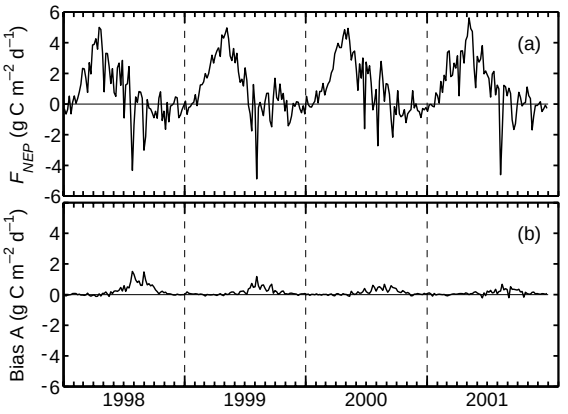

Fig. 6. (a) Five-day average F_{NEP} calculated using the standard method (see text) with $u_{*th} = 0.3\,m\,s^{-1}$ (upper panel) and (b) bias B in F_{NEP} due to applying u_{*th} to the nighttime F_{NEE}. The latter was calculated as F_{NEP} for $u_{*th} = 0.2\,m\,s^{-1}$ minus F_{NEP} for $u_{*th} = 0.3\,m\,s^{-1}$.

more frequent occurrence of low turbulence conditions (see Fig. 4(a)). Furthermore, the months of July, August, and September are the warmest at this site (see Fig. 3) and the calculated respiratory losses from the system are largest for these months.

The regression of the half-hourly energy balance terms using the data for all 4 years resulted in $H + \lambda E = (0.885 \pm 0.004) R_a - (14 \pm 51)\,W\,m^{-2}$ for $u_{*th} = 0.3\,m\,s^{-1}$ (ranges are 95% CI). This lack of energy balance closure of 12% is comparable to that found at other forested sites (Aubinet et al., 2000; Blanken et al., 1998). When energy balance closure was evaluated on an annual basis, the slopes of the regressions were 0.888, 0.879, 0.880, and 0.892 for 1998–2001, respectively, all with an 95% CI of ±0.008. Since these variations were not significantly different at the 95% level from the slope for the regression using all data, we used the single slope value of 0.885 for energy balance correction of data for all 4 years.

Annual estimates of F_{NEP}, P, and R for 1998 calculated using the standard method ($u_{*th} = 0.3\,m\,s^{-1}$), $u_{*th} = 0.2\,m\,s^{-1}$ (bias A), energy balance closure (bias B), and photoinhibition of R_d (bias C) are given in Table 1. The standard method and the photoinhibition correction resulted in the same low annual F_{NEP}. The photoinhibition correction reduced R_d, consequently decreasing $P = -F_{NEE} + R_d$ by the same amount, and leaving F_{NEP} unchanged. In contrast, the energy balance closure correction affected daytime and nighttime fluxes alike, increasing P and R by 12.3 and 12.6%, respectively, consequently increasing the magnitude of F_{NEP} by a similar fraction (11.1%), corresponding to an increase of 30 g C m^{-2} per year. Using a u_{*th} of $0.2\,m\,s^{-1}$ led to an increase in annual F_{NEP} of 90 g C m^{-2} per year. The reduction of u_{*th} for the nighttime data allowed smaller nighttime fluxes into the analysis, which reduced the annual R estimate. This resulted in lower estimates of R_d and hence also lowered the annual P estimate. However, as the reduction in R resulted from reduction during nighttime and daytime it was larger than the reduction of P, which translated into a 33% increase in F_{NEP} (Table 1). The actual bias of the annual F_{NEP} due to the analysis procedure might have been larger than any of the individual biases since more than one bias correction might be required to get the correct estimate.

Table 1
Annual totals of F_{NEP}, P, and R in g C m^{-2} per year for 1998, calculated with the standard method ($u_{*th} = 0.3\,m\,s^{-1}$), with $u_{*th} = 0.2\,m\,s^{-1}$ (bias A), with energy balance closure correction (bias B), and with photoinhibition correction of R_d (bias C)

	Standard	Bias A	Bias B	Bias C
F_{NEP}	270	360	300	270
P	2170	2020	2440	2010
R	1900	1660	2140	1740

4.2.2. Random error

The large uncertainties in the annual F_{NEP} seem to cast doubt on the possibility of any reasonable evaluation of ecosystem behavior based on the EC data. Fortunately, the biases discussed above are systematic and differences between years for a single method can still be statistically significant. Fig. 7 presents the differences between the annual values of F_{NEP}, P, and R for 1999–2001 and those for 1998 for all four methods of analysis. All methods indicated that F_{NEP} values for 1999–2001 were higher than 1998. Maximum F_{NEP} occurred in 2001 for each method. Also, all methods gave the lowest values for P in 1999, and the second lowest for 2001, while R values were similar for the 2 years. Differences between F_{NEP} in 1998 and the other years were greater than the worst case random error estimates given in Table 2 (30 g C m^{-2} per year). In 1999, F_{NEP} was significantly lower than in 2001, while F_{NEP} for 2000 fell between the values for 1999 and 2001 (Fig. 7, Table 2).

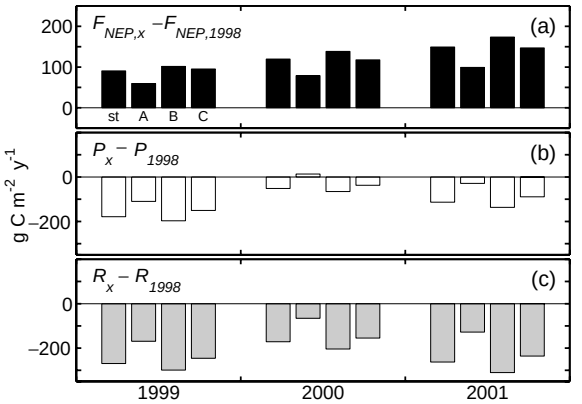

Fig. 7. Differences between the annual values of F_{NEP} (a), P (b), and R (c) for 1999–2001 (x) and those for 1998 calculated with the standard method ($u_{*th} = 0.3\,m\,s^{-1}$), with $u_{*th} = 0.2\,m\,s^{-1}$ (bias A), with energy balance closure correction (bias B), and with photoinhibition correction of daytime respiration (R_d) (bias C).

Table 2
Annual totals of F_{NEP}, P, and R in g C m^{-2} per year calculated using the standard method and the random error estimates from Eqs. (10) and (11) for the annual F_{NEP}

	1998	1999	2000	2001
F_{NEP}	270	360	390	420
ΔF_{NEP} (Eq. (10))	30	30	30	30
ΔF_{NEP} (Eq. (11))	4	4	4	4
P	2170	1990	2120	2060
R	1900	1630	1730	1640

The combined evaluation of bias and random errors shows that the pattern of interannual variability was preserved regardless of the method of analysis, and that differences between annual values were significant even when biases were fairly large. Fig. 5 also supports this point as it shows that the variation of u_{*th} did not change the order of annual F_{NEP} values between years. Therefore, in the remainder of this paper, we use the standard method, i.e., $u_{*th} = 0.3\,m\,s^{-1}$ and no energy balance or photoinhibition correction, to examine the seasonal dynamics and interannual variability of C uptake.

4.3. Seasonal dynamics of carbon uptake

Fig. 8 shows F_{NEE} and u_* for three consecutive sunny days from winter, spring, and summer 1998. All show daytime C uptake (indicated by negative F_{NEE})

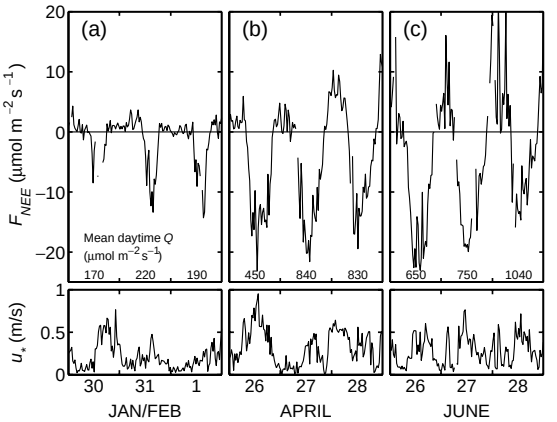

Fig. 8. Three days of F_{NEE} measurements (C uptake by the ecosystem corresponds to negative values), u_*, and mean daytime Q from winter, spring, and summer of 1998.

by the forest stand. During the winter, the periods of uptake were short due to the short length of the day, but F_{NEE} still reached about $-10\,\mu mol\,m^{-2}\,s^{-1}$. Daytime fluxes during spring and summer reached -15 to $-20\,\mu mol\,m^{-2}\,s^{-1}$. High daily Q totals in summer did not necessarily increase downward daytime fluxes, as can be seen for 28 June. This was in part due to high respiration rates, apparent in the nighttime fluxes during the summer period. The two consecutive April nights in Fig. 8, the first with low u_* and small positive F_{NEE} and the second with high u_* and large positive F_{NEE}, are again evidence of a dependence of the nighttime F_{NEE} on u_* as was found in the analysis of the annual F_{NEP} values (see discussion of Fig. 5).

The annual courses of cumulative F_{NEP} in Fig. 9 show a similar pattern for the 4 years. Little net C exchange occurred during November to February. C gain started in February and continued through to the end of July. The maximum rates achieved in March and April varied very little between years and the amount of C sequestered up to the beginning of May was virtually the same for all years at approximately 210 g C m^{-2}. Variation in F_{NEP} in May, June, and July largely determined the difference in annual F_{NEP}. From August to October, F_{NEP} was close to zero or slightly negative. The variability in August and September was not enough to substantially change the relative magnitude of annual F_{NEP} between the years.

Monthly totals of P and R over the 4 years are given in Fig. 10(b) and (c). In spring, R was less than

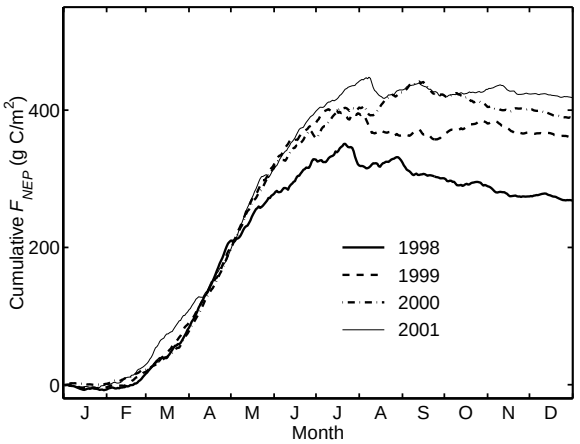

Fig. 9. Annual courses of cumulative F_{NEP} for 1998–2001.

$100\,g\,C\,m^{-2}$ per month as a result of low temperatures, while P quickly increased beyond this value in response to Q (see Fig. 10(b)) and reached a maximum rate of more than $300\,g\,C\,m^{-2}$ per month in July. This resulted in a maximum F_{NEP} of about $120\,g\,C\,m^{-2}$ per month in April and May (see Fig. 10(a)). Monthly R increased to a maximum in August, following the annual course of temperature, corresponding closely to the annual pattern in soil respiration observed by Drewitt et al. (2002). P and R were approximately in balance from August to October, while November and December showed small C losses in all years. Interannual variations in this general pattern occurred mainly in May, June, and July. Above normal temperatures in the first half of 1998 resulted in substantially enhanced R during May through July. P for these months was also enhanced but did not balance the strong increase in R.

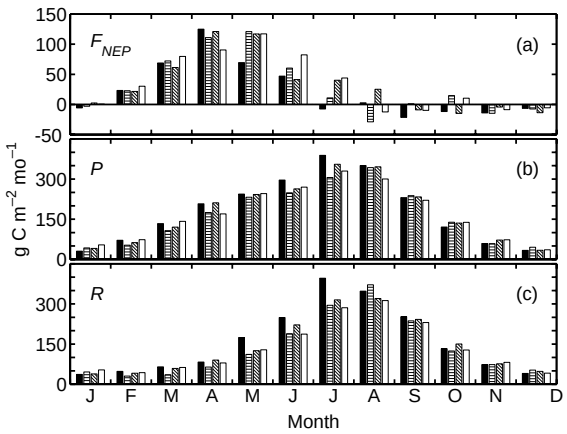

Fig. 10. Monthly totals of F_{NEP}, P, and R calculated using the standard method ($u_{*th} = 0.3\,m\,s^{-1}$). The legend is the same as in Fig. 3.

4.4. Functional relationships and their interannual variability

Table 3 gives the parameter values for the annual relationships of R and T_s (Eq. (6)) and P and Q (Eq. (7)) that were used to fill gaps in the data. The temperature response of R was remarkably similar for 2000 and 2001 where R_{ref} at 10 °C was approximately $5\,\mu mol\,m^{-2}\,s^{-1}$ and Q_{10} was about 5. In 1998, Q_{10} was slightly larger at 5.6, while in 1999, R_{ref} increased to $5.7\,\mu mol\,m^{-2}\,s^{-1}$ and Q_{10} increased to 6.0, indicating that respiration responded most strongly to temperature that year. This, however, did not counter the influence of low temperatures during 1999. In fact, monthly R totals (Fig. 10) were slightly smaller in most months compared to other years. Differences in the annual quantum yield α in the P light response function were not significantly different between years. A_{max} for 1998, 1999, and 2001 was similar at about $25\,\mu mol\,m^{-2}\,s^{-1}$, while in 2000 it increased slightly to $27\,\mu mol\,m^{-2}\,s^{-1}$.

Seasonal variations are expected in the light response of P due to variations in soil moisture and phenological changes in the forest stand, such as root and shoot growth. However, it is difficult to extract these variations from EC data due to the noise added to the biotic signal by atmospheric turbulence. The light response only markedly deviated from the annual relationship during September (Table 3), when values of α increased and values of A_{max} decreased compared to the corresponding annual values. This decrease was most pronounced in 1998, the year with the most severe summer drought, suggesting that this reduction in A_{max} was caused by water stress. Since the light response relationship was used only to fill in missing data during daytime, substituting the annual with the monthly relationship only had a minor influence on the P or F_{NEP} estimates for the month and we decided to use the annual relationship.

Evidence for seasonal variations in the temperature response of soil respiration was found by Drewitt et al. (2002) in chamber measurements of soil respiration at

Table 3
Fitted parameter values for the annual functional relationships for R (Eq. (6)) with R_{ref} at 10 °C and P (Eq. (7)) used in the gap filling procedure

	All year				September	
	R_{ref} (μmol m^{-2} s^{-1})	Q_{10}	α	A_{max} (μmol m^{-2} s^{-1})	α	A_{max} (μmol m^{-2} s^{-1})
1998	4.9 ± 0.3	5.6 ± 0.2	0.07 ± 0.01	25.6 ± 0.3	0.08 ± 0.01	15.6 ± 0.4
1999	5.7 ± 0.3	6.0 ± 0.3	0.05 ± 0.01	24.8 ± 0.4	0.11 ± 0.01	22.0 ± 0.5
2000	5.1 ± 0.3	5.1 ± 0.2	0.06 ± 0.01	27.0 ± 0.4	0.10 ± 0.01	22.7 ± 0.7
2001	5.1 ± 0.3	5.1 ± 0.3	0.06 ± 0.01	25.0 ± 0.4	0.11 ± 0.01	22.4 ± 0.6

Error estimates indicate one standard deviation derived using Eqs. (8) and (9). The Michaelis–Menten relationship fitted to September data only is presented to show the effect of drought on light response.

this site. Q_{10} values listed in Table 3 were generally larger than those found by Drewitt et al. (2002) and were well above the value of 2 that is usually taken as a reasonable physiological estimate for respiratory response to temperature. This was partly due to the use of soil temperature from only one depth to represent the temperature of the whole ecosystem. Furthermore, soil temperature at the 5 cm depth had an amplitude smaller than, for example, that of the air temperature in the canopy space. Relating nighttime F_{NEE} measurements with soil temperatures, therefore, 'compressed' them into a smaller temperature range, leading to an apparent stronger temperature response and higher Q_{10} values.

Given the relatively small interannual variation in the functional relationships, insight can be gained by looking at functional relationships at a longer time scale combining data from all 4 years. Such an assessment of the relationships between monthly totals of P and Q and between monthly totals of R and monthly average air temperatures is given in Fig. 11. It shows that total monthly P was linearly related to Q. The linear nature of the light response on time scales of days and longer is well known (Grace, 1983) and is due to the integration of P over the diurnal cycle. Even though the light response on the half-hourly time scale was well described by the non-linear Michaelis–Menten relationship, the total daily flux was dominated by the maximum fluxes centered around midday. Therefore, daily assimilation was determined by the length of the day, which in turn was approximately proportional to total Q. Hence, the integrated light response was

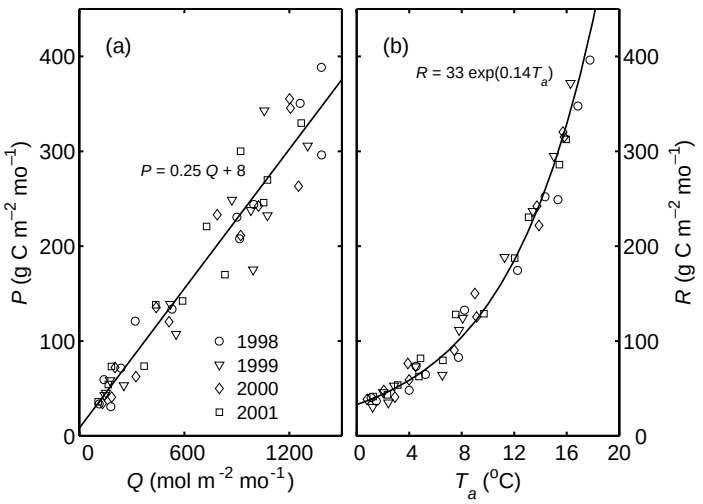

Fig. 11. (a) Relationship between monthly total P and total Q, and (b) between monthly total R and mean T_a.

close to linear. The temperature response of R, on the other hand, lacked a saturation point and consequently was exponential even when data was integrated at a monthly scale. The smaller scatter of monthly R around the regression relationship with temperature compared to the light response regression was partly due to the fact that the daytime portion of the total R had to be calculated from the respiration relationship, rather than measurements, which are more variable due to the noise in the turbulent flux measurement.

The difference in the response of P and R to their driving variables led to a delicate balance in their influence on F_{NEP}. In winter, monthly values of R as well as P were around 50 g C m^{-2} per month. During late summer, when temperatures were highest, R approximately balanced P. In April and May, monthly Q totals were around 1000 mol m^{-2} per month (Fig. 4) and P was about 200–250 g C m^{-2} per month (Fig. 10). Temperatures for these months were between 8 and 12 °C (Fig. 3). The variation in R during this time was considerable (100–200 g C m^{-2} per month) due to the exponential nature of the temperature relationship. Therefore, the annual C balance was very sensitive to temperature variations during these spring months.

4.5. Interannual variability of carbon uptake

The high springtime R in 1998 led to the largest annual value of R for the 4 years (1900 g C m^{-2} per year, see Table 2). This resulted in an annual F_{NEP} of only 270 g C m^{-2} per year despite the fact that the annual P of 2170 g C m^{-2} per year was slightly larger than the 2120 g C m^{-2} per year estimated for 2000 and 2060 g C m^{-2} per year for 2001. In 1999, R was reduced to 1630 g C m^{-2} per year, due to lower temperatures despite the increase in temperature sensitivity mentioned earlier. P was also reduced in 1999 due to low Q, especially in the summer, so that the annual F_{NEP} of 360 g C m^{-2} per year was similar to the following year, when both R and P were relatively high and the annual F_{NEP} was 390 g C m^{-2} per year. Finally, in 2001 annual R and P were reduced. This led to a marginally higher annual F_{NEP} (420 g C m^{-2} per year) compared to the two previous years.

These annual F_{NEP} estimates are comparable to those found by other CO_2 flux monitoring studies of forests in the Pacific Northwest. Anthoni et al. (1999) reported a F_{NEP} of 320 and 270 g C m^{-2} per year by an old-growth stand at Metolius Ridge in 1996 and 1997, respectively. The uncertainty in these values (∼180 g C m^{-2} per year) was also comparable to that derived above, and were equally attributed to uncertainty in P and nighttime R. Anthoni et al. (1999) observed higher R when there was increased precipitation despite similar temperatures in the two summers of their study. These results suggested a shift in temperature response of R similar to that described above for our site in 1999. The authors stressed that they observed C uptake outside the classic growing season, leading to year-round C uptake at their site. In contrast, at our site, in winter, monthly F_{NEP} values were close to zero even though daytime C uptake was observed due to usually mild conditions. A similar annual pattern of net C exchange was reported by Falk et al. (2002) for the Wind River site in southern Washington State, a region with climate conditions similar to those of the east coast of Vancouver Island. Annual F_{NEP} values for the Wind River site ranged from −50 to 210 g C m^{-2} per year with the majority of C uptake occurring during early spring, followed by C loss in summer and little net C exchange in winter. This pattern is markedly different from the behavior of boreal forests, which show small but consistent C losses during the winter. C sequestration is greatest at the beginning and end of the growing season, while it can be inhibited by high temperatures during the summer (Griffis et al., 2003). The El Niño event of 1997/1998 produced an early spring in the boreal region, leading to a longer growing season and greater annual C uptake in a southern boreal aspen forest in Saskatchewan (Black et al., 2000).

5. Conclusions

(1) Interannual variations in annual F_{NEP} did not depend on the analysis method and could be attributed to specific climatic variations when interannual differences exceeded the random variability.
(2) Systematic biases due to the methods of analysis were about 90 g C m^{-2} per year and hence were more important than random error, for which a worst case estimate of 30 g C m^{-2} per year was derived.

(3) The temperature sensitivity of R was similar for 1998, 2000, and 2001, but was higher during the relatively cool La Niña year in 1999. Late summer drought played a minor role in explaining variability in annual F_{NEP}, even though it decreased photosynthetic capacity in September 1998.
(4) A maximum F_{NEP} of about $120\,g\,C\,m^{-2}$ per month occurred during April or May. Interannual variability of monthly F_{NEP} was largest in May, June, and July, causing the annual F_{NEP} of this second-growth Douglas-fir stand established in 1949 to vary between 270 and $420\,g\,C\,m^{-2}$ per year.
(5) The highest annual F_{NEP} occurred in 2001, even though both R and P were slightly reduced. Following the 1997/1998 El Niño event, above-average temperatures led to high annual R in 1998 and consequently to the lowest annual F_{NEP} of the 4 years. Larger scale studies are needed to quantify the contribution of the Pacific Northwest to the global C balance; however, our results at the ecosystem scale are consistent with the observed high rates of increase in CO_2 concentration observed at the global scale following this El Niño event.

Acknowledgements

This research was initially funded by Forest Renewal, BC and continued by Operating and Strategic grants from the Natural Science and Engineering Research Council of Canada. Significant contributions from Fluxnet-Canada and the Canadian Foundation for Innovations are also appreciated. Doug Worthy, Meteorological Service of Canada, provided valuable assistance with calibration gases. Bill Grutzmacher, Steve Lackey, and Al Aalgaard of TimberWest Forest Corp, and Bill Beese of Weyerhaeuser Canada made the operation of our research site on private land possible. Altaf Arain, John Warland, Mike Novak, and David Gaumont-Guay contributed many helpful insights during discussions. Gilbert Ethier, Eva Jork, Scott Krayenhoff, Isla Myers-Smith, Leslie Dampier, and Paul Jassal made many helpful contributions through their work at the site. Last but by no means least the technical assistance provided by Dwaine Young, Andrew Sauter, and Rick Ketler was crucial in keeping this long-term monitoring project going.

References

Anthoni, P.M., Law, B.E., Unsworth, M.H., 1999. Carbon and water vapor exchange of an open-canopied ponderosa pine ecosystem. Agric. For. Meteorol. 95, 151–168.

Anthoni, P.M., Unsworth, M.H., Law, B.E., Irvine, J., Baldocchi, D.D., Van Tuyl, S., Moore, D., 2002. Seasonal differences in carbon and water vapor exchange in young and old-growth ponderosa pine ecosystems. Agric. For. Meteorol. 111, 203–222.

Aubinet, M., Grelle, A., Ibrom, A., Rannik, U., Moncrieff, J., Foken, T., Kowalski, A.S., Martin, P.H., Berbigier, P., Bernhofer, C., Clement, R., Elbers, J., Granier, A., Grunwald, T., Morgenstern, K., Pilegaard, K., Rebmann, C., Snuder, W., Valentini, R., Vesala, T., 2000. Estimates of the annual net carbon and water exchange of forests: the EUROFLUX methodology. Adv. Ecol. Res. 30, 113–176.

Baldocchi, D.D., 2003. Assessing the eddy covariance technique for evaluating carbon dioxide exchange rates of ecosystems: past, present and future. Global Change Biol. 9, 479–492.

Barford, C.C., Wofsy, S.C., Goulden, M.L., Munger, J.W., Hammond Pyle, E., Urbansky, S.P., Hutyra, L., Saleska, S.R., Fitzjarrald, D., Moore, K., 2001. Factors controlling long- and short-term sequestration of atmospheric CO_2 in a mid-latitude forest. Science 294, 1688–1691.

Black, T.A., Chen, W.J., Barr, A.G., Arain, M.A., Chen, Z., Nesic, Z., Hogg, E.H., Neumann, H.H., Yang, P.C., 2000. Increased carbon sequestration by a boreal deciduous forest in years with a warm spring. Geophys. Res. Lett. 27 (9), 1271–1274.

Black, T.A., Den Hartog, G., Neumann, H.H., Blanken, P.D., Yang, P.C., Russell, C., Nexic, Z., Lee, X., Chen, S.G., Staebler, R., Novak, M.D., 1996. Annual cycles of water vapour and carbon dioxide fluxes in and above a boreal aspen forest. Global Change Biol. 2, 219–229.

Blanken, P.D., Black, T.A., Neumann, H.H., den Hartog, G., Yang, P.C., Nesic, Z., Staebler, R., Chen, W., Novak, M.D., 1998. Turbulent flux measurements above and below the overstory of a boreal aspen forest. Boundary-Layer Meteorol. 89, 109–140.

Brooks, A., Farquhar, G.D., 1985. Effect of temperature on the CO_2/O_2 specificity of ribulose-1,5-bisphosphate carboxylase/oxygenase and the rate of respiration in the light. Planta 165, 397–406.

Chen, W.J., Black, T.A., Yang, P.C., Barr, A.G., Neumann, H.H., Nesic, Z., Blanken, P.D., Novak, M.D., Eley, J., Ketler, R.J., Cuencas, R., 1999. Effects of climatic variability on the annual carbon sequestration by a boreal aspen forest. Global Change Biol. 5 (1), 41–53.

Cubasch, U., Meehl, G.A., Boer, G.J., Stouffer, R.J., Dix, M., Noda, A., Senior, C.A., Raper, S., Yap, K.S., 2001. Projections of future climate change. In: Houghton, J.T., et al. (Eds.), Climate Change 2001: The Scientific Basis. Cambridge University Press, Cambridge, pp. 525–582.

Drewitt, G.B., Black, T.A., Nesic, Z., Humphreys, E.R., Jork, E.M., Swanson, R., Ethier, G.J., Griffis, T., Morgenstern, K., 2002. Measuring forest floor CO_2 fluxes in a Douglas-fir forest. Agric. For. Meteorol. 110 (4), 299–317.

Falge, E., Baldocchi, D., Olson, R., Anthoni, P., Aubinet, M., Bernhofer, C., Burba, G., Ceulemans, R., Clement, R., Dolman, H., Granier, A., Gross, P., Grünwald, T., Hollinger, D., Jensen, N.-O., Katul, G., Keronen, P., Kowalski, A., Lai, C., Law, B.E., Meyers, T., Moncrieff, J., Moors, E., Munger, W.J., Pilegaard, K., et al., 2001. Gap filling strategies for defensible annual sums of net ecosystem exchange. Agric. For. Meteorol. 107 (1), 43–69.

Falge, E., Baldocchi, D., Olson, R., Anthoni, P., Aubinet, M., Bernhofer, C., Burba, G., Ceulemans, R., Clement, R., Dolman, H., Granier, A., Gross, P., Grünwald, T., Hollinger, D., Jensen, N.-O., Katul, G., Keronen, P., Kowalski, A., Ta Lai, C., Law, B.E., Meyers, T., Moncrieff, J., Moors, E., Munger, W.J., Pilegaard, K., et al., 2001. Gap filling strategies for long term energy flux data sets. Agric. For. Meteorol. 107 (1), 71–77.

Falk, M., Paw, U.K.T., Schroeder, M., 2002. Long-term carbon and energy fluxes for an old-growth rainforest. International Congress of Biometeorology, Kansas City, pp. 16C.2.

Finnigan, J.J., Clement, R., Mahli, Y., Leuning, R., Cleugh, H.A., 2003. A re-evaluation of long-term flux measurement techniques. Part I. Averaging and coordinate rotation. Boundary-Layer Meteorol. 107, 1–48.

Gholz, H.L., 1982. Environmental limits on aboveground net primary production, leaf area, and biomass in vegetation zones of the Pacific Northwest. Ecology 63 (2), 469–481.

Goulden, M.L., Daube, B.C., Song Miao, F., Sutton, D.J., Bazzaz, A., Munger, J.W., Wofsy, S.C., 1997. Physiological responses of a black spruce forest to weather. J. Geophys. Res. 102 (D24), 28987–28996.

Goulden, M.L., Munger, W., Fan, S.M., Daube, B.C., 1996. Measurements of carbon sequestration by long-term eddy covariance: methods and a critical evaluation of accuracy. Global Change Biol. 2, 169–182.

Grace, J., 1983. Plant–Atmosphere Relationships. Chapman & Hall, London.

Grace, J., Lloyd, J., McIntyre, J., Miranda, A.C., Meir, P., Miranda, H.S., Nobre, C., Moncrieff, J., Massheder, J., Malhi, Y., Wright, I., Gash, J., 1995. Carbon dioxide uptake by an undisturbed tropical rain forest in southwest Amazonia, 1992 to 1993. Science 270, 778–780.

Greco, S., Baldocchi, D.D., 1996. Seasonal variations of CO_2 and water vapour exchange rates over a temperate deciduous forest. Global Change Biol. 2, 183–197.

Griffis, T.J., Black, T.A., Morgenstern, K., Barr, A.G., Nesic, Z., Drewitt, G.B., Gaumont-Guay, D., McCaughey, J.H., 2003. Ecophysiological controls of the carbon balance of three southern boreal forests. Agric. For. Meteorol. 117, 53–71.

Hollinger, D.Y., Kelliher, F.M., Byers, J.N., Hunt, J.E., McSeveny, T.M., Weir, P.L., 1994. Carbon dioxide exchange between an undisturbed old-growth temperate forest and the atmosphere. Ecology 75 (1), 134–150.

Humphreys, E.R., Black, T.A., Ethier, G.J., Drewitt, G.B., Spittlehouse, D.L., Jork, E.-M., Nesic, Z., Livingston, N.J., 2003. Annual and seasonal variability of sensible and latent heat fluxes above a coastal Douglas-fir forest, British Columbia, Canada. Agric. For. Meteorol. 115, 109–125.

Janssens, I.A., Lankreijer, H., Matteucci, G., Kowalski, A.S., Buchmann, N., Epron, D., Pilegaard, K., Kutsch, W., Longdoz, B., Grünwald, T., Montagnani, L., Dore, S., Rebmann, C., Moors, E.J., Grelle, A., Rannik, Ü., Morgenstern, K., Clement, R., Guðmundsson, J., Minerbi, S., Berbigier, P., Ibrom, A., Moncrieff, J., Aubinet, M., Bernhofer, C., et al., 2001. Productivity and disturbance overshadow temperature in determining soil and ecosystem respiration across European forests. Global Change Biol. 7, 269–278.

Jarvis, P.G., Dolman, A.J., Schulze, E.D., Matteucci, G., Kowalski, A.S., Ceulemans, R., Rebmann, C., Moors, E.J., Granier, A., Gross, P., Jensen, N.O., Pilegaard, K., Lindroth, A., Grelle, A., Bernhofer, C., Grunwald, T., Aubinet, M., Ceulemans, R., Kowalski, A.S., Vesala, T., Rannik, U., Berbigler, P., Loustau, D., Guomundsson, J., Thorgeirsson, H., et al., 2001. Carbon balance gradient in European forests: should we doubt 'surprising' results? A reply to Piovesan & Adams. J. Veg. Sci. 12, 145–150.

Kaimal, J.C., Finnigan, J.J., 1994. Atmospheric Boundary Layer Flows: Their Structure and Measurement. Oxford University Press, New York.

Keeling, C.D., Chin, J.F.S., Whorf, T.P., 1996. Increased activity of northern vegetation inferred from atmospheric CO_2 observations. Nature 382, 146–149.

Keyes, M.R., Grier, C.C., 1981. Above- and below-ground net production in 40-year-old Douglas-fir stands on low and high productivity sites. Can. J. For. Res. 11, 599–605.

Lindroth, A., Grelle, A., Moren, A.S., 1998. Long-term measurements of boreal forest carbon balance reveal large temperature sensitivity. Global Change Biol. 4 (4), 443–450.

Lloyd, J., Shibistova, O., Zolotoukhine, D., Kolle, O., Arneth, A., Wirth, C., Styles, J.M., Tchebakova, N.M., Schulze, E.-D., 2002. Seasonal and annual variations in the photosynthetic productivity and carbon balance of a Siberian pine forest. Tellus 54B, 590–610.

Lloyd, J., Taylor, J.A., 1994. On temperature dependence of soil respiration. Funct. Ecol. 8, 315–323.

Manly, B.F.J., 1997. Randomization, Bootstrap and Monte Carlo Methods in Biology. Chapman & Hall, London.

Meidinger, D.V., Pojar, J., 1991. Ecosystems of British Columbia. British Columbia Ministry of Forests, Research Branch, Victoria, BC.

Meteorological Service of Canada, 2002. Canadian Climate Normals 1971–2000 (Website: http://www.msc-smc.ec.gc.ca/climate/climate_normals/index_e.cfm).

Mitchell, J.F.B., Karoly, D.J., Hegerl, G.C., Zwiers, F.W., Allen, M.R., Marengo, J., 2001. Detection of climate change and attribution of causes. In: Houghton, J.T., et al. (Eds.), Climate Change 2001: The Scientific Basis. Cambridge University Press, Cambridge, pp. 525–582.

Moncrieff, J.B., Mahli, Y., Leuning, R., 1996. The propagation of errors in long-term measurements of land-atmosphere fluxes of carbon and water. Global Change Biol. 2, 231–240.

Pilegaard, K., Hummelshoj, P., Jensen, N.O., Chen, Z., 2001. Two years of continuous CO_2 eddy-flux measurements over a Danish beech forest. Agric. For. Meteorol. 107, 29–41.

Piovesan, G., Adams, J.M., 2000. Carbon balance gradient in European forests: interpreting EUROFLUX. J. Veg. Sci. 11, 923–926.

Prentice, I.C., Farquhar, G.D., Fasham, M.J.R., Goulden, M.L., Heimann, M., Jaramillo, V.J., Kheshgi, H.S., Le Quéré, C., Scholes, R.J., Wallace, D.W.R., 2001. The carbon cycle and atmospheric carbon dioxide. In: Houghton, J.T., et al. (Eds.), Climate Change 2001: The Scientific Basis. Cambridge University Press, Cambridge, pp. 183–238.

Price, D.T., Black, T.A., 1990. Effects of short-term variation in weather on diurnal canopy CO_2 flux and evapotranspiration of a juvenile Douglas-fir stand. Agric. For. Meteorol. 50, 139–158.

Price, D.T., Black, T.A., 1991. Effects of summertime changes in weather and root-zone soil water storage on canopy CO_2 flux and evapotranspiration of two juvenile Douglas-fir stands. Agric. For. Meteorol. 53, 303–323.

Randerson, J.T., Field, C.B., Fung, I.Y., Tans, P.P., 1999. Increases in early season ecosystem uptake explain recent changes in the seasonal cycle of atmospheric CO_2 at high northern latitudes. J. Geophys. Res. 26, 2765–2768.

Schimel, D.S., House, J.I., Hibbard, K.A., Bousquet, P., Ciais, P., Peylin, P., Braswell, B.H., Apps, M.J., Baker, D., Bondeau, A., Canadell, J., Churkina, G., Cramer, W., Denning, A.S., Field, C.B., Friedlingstein, P., Goodale, C., Heimann, M., Houghton, R.A., Melillo, J.M., Moore, B., Murdiyarso, D., Noble, I., Pacala, S.W., Prentice, I.C., et al., 2001. Recent patterns and mechanisms of carbon exchange by terrestrial ecosystems. Nature 414, 169–172.

Shabbar, A., Bonsal, B., Khandekar, M., 1997. Canadian precipitation patterns associated with the Southern Oscillation. J. Climate 10 (12), 3016–3027.

Shabbar, A., Khandekar, M.L., 1996. The impact of El Nino/Southern Oscillation on the temperature field over Canada. Atmosphere-Ocean 34 (2), 401–416.

Squires, G.L., 1968. Practical Physics. McGraw-Hill, Maidenhead.

Tabachnick, B.G., Fidell, L.S., 2001. Using Multivariate Statistics. Allyn and Bacon, Boston, MA.

Tanner, C.B., Thurtell, G.W., 1969. Anemoclinometer measurements of Reynolds stress and heat transport in the atmospheric surface layer. ECOM 66-G22-F. University of Wisconsin, Madison, WI.

Twine, T.E., Kustas, W.P., Norman, J.M., Cook, D.R., Houser, P.R., Meyers, T.P., Prueger, J.H., Starks, P.J., Wesely, M.L., 2000. Correcting eddy-covariance flux underestimates over a grassland. Agric. For. Meteorol. 103, 279–300.

Valentini, R., Matteucci, G., Dolman, A.J., Schulze, E.D., Rebmann, C., Moors, E.J., Granier, A., Gross, P., Jensen, N.O., Pilegaard, K., Lindroth, A., Grelle, A., Bernhofer, C., Grunwald, T., Aubinet, M., Ceulemans, R., Kowalski, A.S., Vesala, T., Rannik, U., Berbigler, P., Loustau, D., Guomundsson, J., Thorgeirsson, H., Ibrom, A., Morgenstern, K., et al., 2000. 2000. Respiration as the main determinant of carbon balance in European forests. Nature 404 (6780), 861–865.

Villar, R., Held, A.A., Merino, J., 1994. Dark leaf respiration in light and darkness of an evergreen and a deciduous plant species. Plant Phys. 107, 421–427.

Waring, R.H., Franklin, J.F., 1979. Evergreen coniferous forests of the Pacific Northwest. Science 204, 1380–1386.

Webb, E.K., Pearman, G.I., Leuning, R., 1980. Correction of flux measurements for density effects due to heat and water vapor transfer. Q. J. R. Meteorol. Soc. 106, 85–100.

Wesely, M.L., Hart, R.L., 1985. Variability of short term eddy-correlation estimates of mass exchange. In: Hutchinson, B.A., Hicks, B.B. (Eds.), The Forest–Atmosphere Interaction. D. Reidel, Dordrecht, pp. 591–612.

Yang, P.C., Black, T.A., Neumann, H.H., Novak, M.D., Blanken, P.D., 1999. Spatial and temporal variability of CO_2 concentration and flux in a boreal aspen forest. J. Geophys. Res. 104 (D22), 27,653–27,661.